The role of the support in the oxidative destruction of chlorobenzene on Pt/zeolite catalysts: an FT-IR investigation

Salvatore Scirè* and Simona Minicò

Dipartimento di Scienze Chimiche, Università di Catania, V. le A. Doria, 6, 95125 Catania (Italy)

Received 3 July 2003; accepted 24 September 2003

The deep oxidation of chlorobenzene was investigated over Pt/H-ferrierite and Pt/H-ZSM5 catalysts. Catalytic results showed that Pt/zeolite samples exhibit higher activity and lower by-products formation than Pt/γ-Al_2O_3, tested for comparison. Pt/H-ferrierite resulted to be the most favorable system as it leads to the lowest formation of noxious polychlorinated benzenes. The present FT-IR investigation pointed out that the support significantly affects the combustion of chlorobenzene over Pt/zeolite catalysts, support acidity directing the activity of the system and pore structure of the zeolite determining the level and the distribution of polychlorinated compounds.

KEY WORDS: catalytic combustion; chlorobenzene; platinum; H-ZSM5; H-ferrierite; FT-IR.

1. Introduction

Among all volatile organic compounds, chlorinated aromatics require special attention due to their toxicity, high stability and widespread application in industry [1,2]. The current technology for the total oxidation of chlorinated volatile organic compounds (Cl-VOCs) involves incineration at extremely high temperatures (>1000 °C). This process, however, requires large energy input and can lead to highly toxic by-products, such as dioxins and dibenzofurans, which can be formed by incomplete combustion [1,2]. Catalytic combustion can be considered as an interesting alternative to thermal oxidation, being advantageous because of its low temperature of operation (<500 °C), low energy consumption and reduced formation of noxious by-products [3,4]. The interaction of the catalyst with chlorine is the main problem met in the design of catalytic systems for the combustion of Cl-VOCs. The optimal catalyst for this reaction should be active, stable and, above all, highly selective to CO_2, H_2O and HCl (this latter compound being easily eliminated from the stream by washing), limiting the formation of other environmentally hazardous organic compounds.

Metal oxides or supported noble metals are the most investigated catalysts for the combustion of Cl-VOCs [1,2,5–16]. Generally, noble metals (platinum and palladium) exhibit high activity for the oxidation of many VOCs. However, on these metals, chlorination of organic compounds besides their oxidation can also occur, leading to considerable amounts of polychlorinated compounds [1,5,6], which are more toxic and recalcitrant than the starting material. Metal oxides are much less expensive than noble metals, but they are also inherently less active. Moreover, with metal oxides, the formation of volatile metaloxychlorides is a serious problem, leading to a relevant catalyst deactivation [5,6]. U_3O_8 has been reported as the only exception, but an industrial application of this catalyst requires special procedures for its safe handling due to chemical toxicity considerations [1].

During last years, zeolites have gained interest as potential catalysts for several reactions of environmental interest [17]. Some papers dealt with the catalytic combustion of Cl-VOCs over zeolite-based catalysts [11–16]. H-zeolites (H-ZSM5, H-Y and H-MOR) exhibited high activity for the oxidative destruction of 1,2-dichloroethane and trichloroethylene [11,12]. Metal-loaded zeolite catalysts have been found to be active in the catalytic oxidation of methylene chloride (Cr-Y [13]) and chlorobenzene (Pd-Y [14]). More recently, we have investigated the deep oxidation of chlorobenzene over platinum catalysts supported on various H-type zeolites [15,16]. We have found that catalytic performances of the Pt/zeolite system toward the chlorobenzene combustion strongly depend on the type of zeolite used [15,16]. In particular, Pt/H-Y and Pt/H-β resulted to be more active than Pt/H-ZSM5 and Pt/H-ferrierite, these two latter samples however producing considerably lower amount of polychlorinated benzenes ($PhCl_x$) as by-products [15]. These results were explained by us assuming that zeolite structure can induce a product shape selectivity effect, a lower size of channels hindering the further chlorination of chlorobenzene to $PhCl_x$ [15,16]. In order to confirm this hypothesis here, we report a study on the accessibility of chloro- and dichlorobenzenes into the zeolite pores by means of FT-IR spectroscopy.

* To whom correspondence should be addressed.
E-mail: sscire@dipchi.unict.it

1011-372X/03/1200–0199/0 © 2003 Plenum Publishing Corporation

2. Experimental

2.1. Catalysts preparation

Platinum (0.5 wt%) catalysts were prepared by incipient wetness impregnation of supports with appropriate amounts of aqueous solution of H_2PtCl_6 (Alfa Aesar). Two H-ferrierites (Zeolyst, SiO_2/Al_2O_3 ratios of 20 and 55, surface area: 400 m^2/g), one H-ZSM5 (Zeolyst, SiO_2/Al_2O_3 ratio of 30, surface area: 400 m^2/g), and one γ-Al_2O_3 (Harshaw, surface area: 100 m^2/g) were used as supports. Code of samples, together with support used and SiO_2/Al_2O_3 ratios of zeolites, are reported in table 1.

2.2. FT-IR measurements

For FT-IR studies, the powdered samples were compressed into thin self-supporting discs of about 25 mg cm^{-2} and 0.1 mm thick. The disc was placed in an IR cell, which allows thermal treatments in vacuum or in a controlled atmosphere. In the cell, all samples were reduced in pure H_2 at 450 °C for 30 min, evacuated at the same temperature for 1 h and finally cooled at room temperature. Commercial (all Fluka) chlorobenzene (PhCl), 1,4-dichlorobenzene (*p*-$PhCl_2$) and 1,3-dichlorobenzene (*m*-$PhCl_2$) have been vaporized in vacuum and adsorbed from the gas phase. Spectra were recorded with a Perkin Elmer System 2000 FT-IR spectrophotometer with a resolution of 2 cm^{-1}. Data are reported as difference spectra obtained by subtracting the spectrum of the sample before the admission of the adsorbate and are normalized to the same amount of catalysts per cm^2.

2.3. Catalysts' characterization

The acid properties of catalysts were determined by temperature programmed desorption of ammonia (NH_3-TPD) and FT-IR of adsorbed pyridine. TPD experiments were carried out in a quartz U-shape reactor in a flow of helium with a constant heating rate of 10 °C min^{-1}. The desorbed products were detected by a quadrupole mass spectrometer (Sensorlab VG Quadrupoles). Before TPD, all samples were reduced in flowing H_2 for 1 h at 450 °C, maintained at this temperature for 1 h in flowing helium and then cooled at room temperature, always in a flow of helium. FT-IR of pyridine was carried out using the FT-IR equipment described above. Commercial pyridine (Fluka) had been vaporized in vacuum and adsorbed from the gas phase. Subsequent evacuation at 250 °C was then performed in order to remove physisorbed pyridine.

Catalysts were also characterized by H_2 chemisorption, measured in a static system operating at room temperature. Before the measurements, the samples have been reduced in H_2 at 450 °C for 1 h, outgassed at 450 °C for 1 h and then cooled at room temperature.

H/Pt ratio and total amount of adsorbed ammonia of samples are reported in table 1.

Table 1
Code and physicochemical properties of supported platinum samples

Code	Support	SiO_2/Al_2O_3 ratio	H/Pt ratio	NH_3 adsorbed (mmol/g)
PtAl	γ-Al_2O_3	–	0.10	–
PtFER20	H-ferrierite	20	0.09	1.73
PtFER55	H-ferrierite	55	0.05	1.01
PtMFI30	H-ZSM5	30	0.08	1.16

2.4. Catalytic activity measurements

Catalytic activity tests were carried out in a fixed-bed reactor at atmospheric pressure in the 200–550 °C range, using 0.1 g of catalyst. Chlorobenzene (PhCl) was fed to the reactor by a carrying gas of helium flow through a saturator maintained at 2.8 °C, and then mixed with O_2 and helium before reaching the catalyst. The reactant mixture was 10% O_2 and 2000 ppm PhCl diluted with helium. The total gas flow was 44.3 cc/min with a GHSV of 18 600 h^{-1}. The reaction products were analyzed using two on-line gas chromatographs, one equipped with FID detector and HP-INNOWax column for the analysis of PhCl and $PhCl_x$, and the other with TCD detector and Octoil S at 3% on silica gel column for the CO/CO_2 analysis. Tubing and injection valves were heated at 200 °C to prevent condensation of products. For all experiments, CO_2 was the main carbon-containing product, very small amounts of CO were found only at low conversions. The carbon balance was always higher than 97%. Before catalytic runs, all samples were reduced at 450 °C in H_2 for 1 h and then calcined in air at the same temperature for 3 h. Preliminary runs carried out at different flow rates showed the absence of external diffusional limitations. The absence of internal diffusion limitations was verified by running experiments with crushed pellets at different grain size.

3. Results

3.1. FT-IR of adsorbed chlorobenzene and dichlorobenzenes

An FT-IR study of adsorbed chlorobenzene and dichlorobenzenes has been performed in order to obtain information on the accessibility of these molecules into the zeolite channels. Figure 1 shows the subtraction spectra, in the 3800–3000 cm^{-1} region, relative to PhCl, *p*-$PhCl_2$ and *m*-$PhCl_2$ on the PtMFI30 sample, together with the spectrum of the sample before admission of the

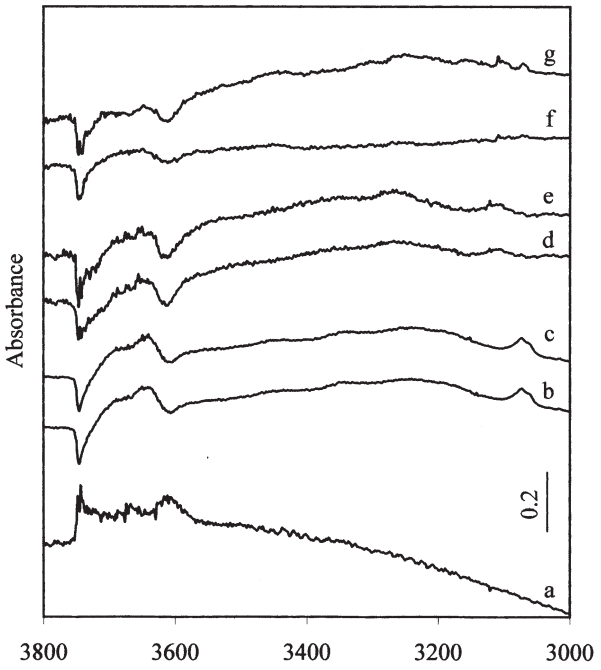

Figure 1. FT-IR spectrum of the PtMFI30 sample (a) before admission of the organic molecule and subtraction spectra (b–g) after contact at room temperature with vapors of (b) PhCl, (d) *p*-$PhCl_2$ and (f) *m*-$PhCl_2$ and after 15 min contact at 300 °C with vapors of (c) PhCl, (e) *p*-$PhCl_2$ and (g) *m*-$PhCl_2$.

organic molecule. The spectrum of PtMFI30 (spectrum a) presents two main bands at 3746 and 3610 cm^{-1}. Two small bands, respectively at ca. 3730 and 3670 cm^{-1}, can also be observed. According to the literature [18,19], the band at 3746 cm^{-1} can be attributed to terminal silanol groups exposed at the external surface of the H-ZSM5, the band at 3730 cm^{-1} is assigned to silanols located in the internal pores of the zeolite in defect sites, the band at 3670 cm^{-1} is related to OHs of extra-framework alumina and finally the 3610 cm^{-1} band is associated with the acidic bridging Si-OH-Al groups. Considering that most of the bridging OHs are located in the internal cavities of the zeolite, the portion of external cavities being very low (<5%), the 3610 cm^{-1} band can be used to get information on the accessibility into zeolitic pores of molecules able to interact with hydroxy groups.

Exposure at room temperature to PhCl vapors results in the disappearance of bands relative to OH groups of the H-ZSM5 zeolite, as well evidenced by negative bands at 3746 and 3610 cm^{-1} in the subtraction spectrum (spectrum b). Correspondingly, new bands arise, mainly one near 3630 cm^{-1}, owing to perturbed terminal silanols interacting with chlorobenzene [19], and a very broad one, in the 3500–3200 cm^{-1} region, associated with bridging OH groups H-bonded with PhCl [19]. The appearance of distinct components in this latter band (the most intense at ca. 3230 cm^{-1}) suggests the presence of bridging OH groups with different acidities [19]. Finally, it must be noted that typical bands in the range 3100–3050 cm^{-1}, due to aromatic CH stretching vibrations of chlorobenzene [20], also become clearly visible in the spectrum upon contact with PhCl.

Upon adsorption of *p*-$PhCl_2$ vapors at room temperature on PtMFI30 (spectrum d), we observe, like for PhCl, an almost total disappearance of both terminal and bridging OH bands of the zeolite and the growth of the corresponding bands of perturbed OHs (one at ca. 3630 cm^{-1} and the other, very broad, in the 3500–3200 cm^{-1} range with the main maximum at ca. 3260 cm^{-1}), together with those of CH stretching vibrations of adsorbed *p*-$PhCl_2$ (near 3100 cm^{-1}). No substantial changes in the spectrum occurred by treatment at higher temperatures both in the case of PhCl (spectrum c) and *p*-$PhCl_2$ (spectrum e), in agreement with the fact that practically all hydroxy groups have been consumed by the adsorbate, already at room temperature. Above FT-IR data point out that chlorobenzene and *p*-dichlorobenzene interact with both bridging (mostly internal) and terminal (external) OHs of H-ZSM5. The interaction with bridging OH groups is stronger than with terminal ones, as evidenced by the higher shift of the Si-OH-Al band ($\Delta\nu_{OH} \approx 200$–$400\ cm^{-1}$) compared to that of Si-OHs ($\Delta\nu_{OH} \approx 115\ cm^{-1}$). This is evidence of the stronger acidity of bridging OHs [19]. These FT-IR results indicate that both PhCl and *p*-PhCl enter easily the channels of H-ZSM5, strongly interacting with internal acidic OHs.

When PtMFI30 is put in contact at room temperature with *m*-$PhCl_2$ vapors (spectrum f), it can be noted that all terminal silanols interact with *m*-$PhCl_2$, whereas only a small part of internal OHs are perturbed by the organic molecule. The entrance of *m*-$PhCl_2$ is sensibly more abundant when contact is carried out at a higher temperature (300 °C), as evidenced (spectrum g) by the clear negative band at 3610 cm^{-1} associated with the positive broad band at a lower frequency (3500–3200 cm^{-1} region). The CH-stretching vibrations of adsorbed *m*-$PhCl_2$ also become visible at this temperature. This behavior indicates that the access of *m*-$PhCl_2$ in the internal sites of H-ZSM5 is somehow restricted, being more difficult compared to that of *p*-$PhCl_2$ and PhCl.

Figure 2 reports the subtraction spectra, in the 3800–3000 cm^{-1} region, relative to PhCl, *p*-$PhCl_2$ and *m*-$PhCl_2$ on the PtFER20 sample, together with the spectrum of the sample before admission of the organic molecule. The FT-IR spectrum of PtFER20 (spectrum a) shows two intense bands at 3746 and 3604 cm^{-1}, attributed respectively to external OH groups (3746 cm^{-1}) and to bridging Si-OH-Al sites mostly located in the internal cavities of the zeolite (3604 cm^{-1}) [19]. After exposure at room temperature to vapors of PhCl (spectrum b), *p*-$PhCl_2$ (spectrum d) or *m*-$PhCl_2$ (spectrum f), the band at 3746 cm^{-1} fully disappears and a new band at 3640 cm^{-1} arises. The

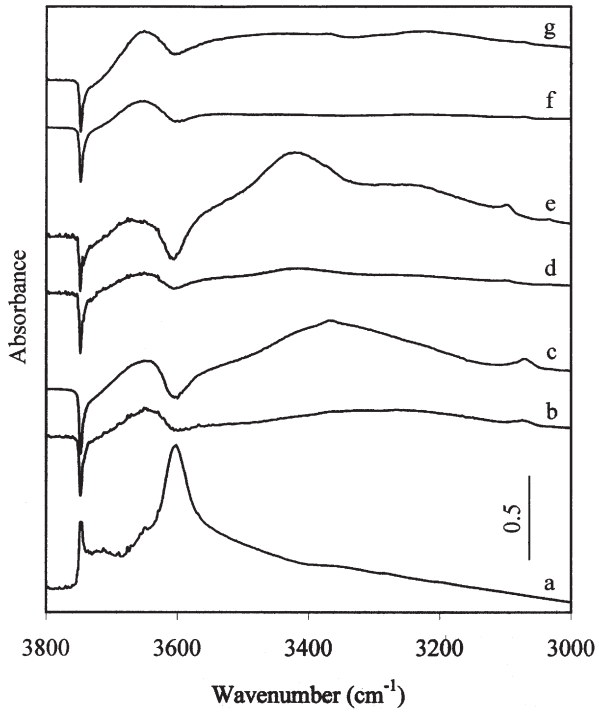

Figure 2. FT-IR spectrum of the PtFER20 sample (a) before admission of the organic molecule and subtraction spectra (b–g) after contact at room temperature with vapors of (b) PhCl, (d) *p*-$PhCl_2$ and (f) *m*-$PhCl_2$ and after 15 min contact at 300 °C with vapors of (c) PhCl, (e) *p*-$PhCl_2$ and (g) *m*-$PhCl_2$.

band at 3604 cm^{-1} is instead not perturbed or is perturbed to a very low extent by contact with all investigated chloroaromatic compounds. This behavior indicates that at room temperature chloro- and dichlorobenzenes interact with external OH groups of H-ferrierite, being substantially unable to reach the internal cavities of this zeolite. When the contact with the organic molecule is carried out at higher temperature (300 °C), both PhCl and *p*-$PhCl_2$ appear to perturb to a higher extent the internal OHs of the ferrierite as shown in the difference spectra (spectra c and e, respectively for PhCl and *p*-$PhCl_2$) by the evident negative band at ca. 3604 cm^{-1}, accompanied by a positive broad band at lower frequency (centered at ca. 3350 cm^{-1} in the case of PhCl and at 3420 cm^{-1} for *p*-$PhCl_2$). The CH-stretching vibrations of the corresponding chloroaromatic compound (near 3100 cm^{-1}) also become noticeable. It is interesting to note, however, that at high temperatures, only a fraction of internal OHs of ferrierite reacts with PhCl and *p*-$PhCl_2$, indicating that only part of cavity OHs can be involved in such an interaction. In the case of the *meta*-dichlorobenzene isomer, the internal OHs of the ferrierite are very slightly perturbed even when *m*-$PhCl_2$ is contacted at high temperature (spectrum g), thus denoting that the entrance of this molecule into ferrierite pores is mostly prevented.

3.2. Catalytic activity

Figure 3 reports the conversion curves for chlorobenzene combustion and the yields to $PhCl_x$ as a function of the reaction temperature over supported platinum catalysts. On the alumina supported platinum sample (PtAl), the reaction starts above 250 °C, reaches 50% conversion at 350 °C and approaches completion at ca. 450 °C. Platinum samples supported on zeolites (PtMFI30, PtFER20 and PtFER55) exhibit higher activity compared to the PtAl sample. The order of activity is PtFER20 ≅ PtMFI30 > PtFER55 > PtAl. From the figure, it is also possible to observe that on all Pt-loaded samples polychlorinated benzenes are

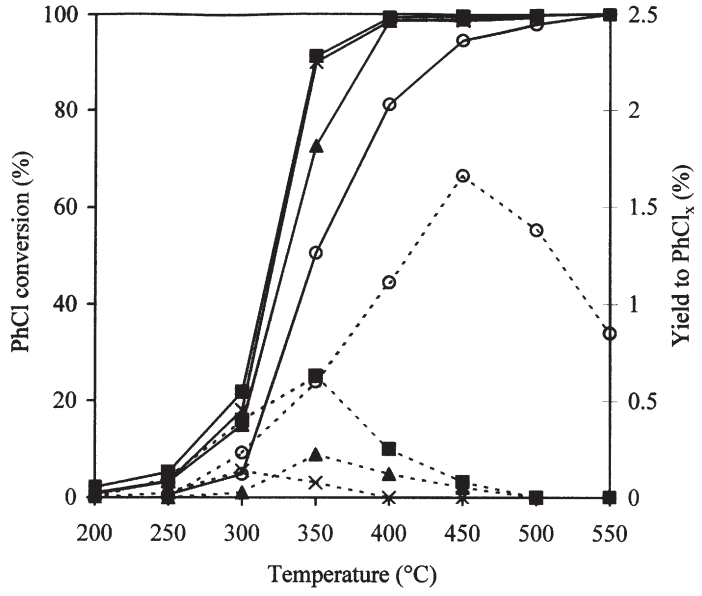

Figure 3. PhCl conversions (full line) and yields to $PhCl_x$ (dotted line) as a function of reaction temperatures over PtAl (○), PtMFI30 (■), PtFER20 (×) and PtFER55 (▲) samples.

formed. The highest level of $PhCl_x$ is found on PtAl (yield to $PhCl_x$ of 1.7%), whereas the formation is sensibly lower on Pt/zeolite catalysts, Pt/H-ferrierite samples producing the lowest $PhCl_x$ amount (>0.3%). It must be reminded that on pure supports (alumina and zeolites) the oxidation of PhCl has been found to occur at much higher temperatures (light-off >400 °C) without substantial formation of $PhCl_x$. This clearly indicates that platinum strongly improves the oxidation activity of oxides, but it is also directly involved in the formation of polychlorinated benzenes [5,6]. Figure 3 shows that the output of $PhCl_x$ reaches a maximum at 450 °C for PtAl and in the 300–350 °C range for zeolite supported platinum samples. From a practical point of view, it is noteworthy that on all zeolite supported samples the production of $PhCl_x$ is almost nil at $T > 450$ °C (temperature at which PhCl is completely converted), whereas on PtAl samples the level of polychlorinated compounds still remains important (0.9%) up to the maximum temperature investigated (550 °C).

Concerning the $PhCl_x$ distribution, it must be underlined that during the conversion of chlorobenzene over PtAl, the formation of the full spectrum of $PhCl_x$ was observed. Dibenzodioxins and dibenzofurans were never found. At reaction temperatures of 350–400 °C, dichlorobenzene isomers were predominant over all $PhCl_x$, the amount of $PhCl_2$ following the order *m*-$PhCl_2$ > *p*-$PhCl_2$ > *o*-$PhCl_2$. On increasing the reaction temperature, the percentage of $PhCl_2$ sensibly decreased in favor of higher polychlorobenzenes, $PhCl_3$, resulting in the most abundant $PhCl_x$ (1,2,4-trichlorobenzene was always the major $PhCl_3$) at 450–500 °C. The above trend in the $PhCl_x$ formation is in accordance with data reported in the literature over a 2 wt% Pt/γ-Al_2O_3 catalyst [5]. On PtMFI30, the formation of $PhCl_x$ is almost limited to $PhCl_2$ isomers with a small amount of $PhCl_3$ and no higher $PhCl_x$ detected at any investigated temperature. On both Pt/H-ferrierite samples, $PhCl_2$ isomers were the only $PhCl_x$ ever observed. It is noteworthy that, different from that observed over Pt/γ-Al_2O_3, the *p*-isomer was always the most abundant dichlorobenzene formed on all Pt/zeolite catalysts. The preferential formation of the *p*-isomer was much more evident on Pt/H-ferrierite samples.

3.3. Characterization of catalysts' acidity

An FT-IR investigation of adsorbed pyridine was performed in order to characterize the acid properties of tested catalysts. It is well known that ring stretching vibrations of pyridine (1400–1700 cm^{-1} region) are the most informative modes on the nature and strength of acid sites [21]. Bands at ca. 1640 and 1540 cm^{-1} are characteristic of pyridinium ions (adsorption on Brønsted sites), whereas bands in the 1600–1630 cm^{-1} and 1440–1455 cm^{-1} regions are specific of coordinatively

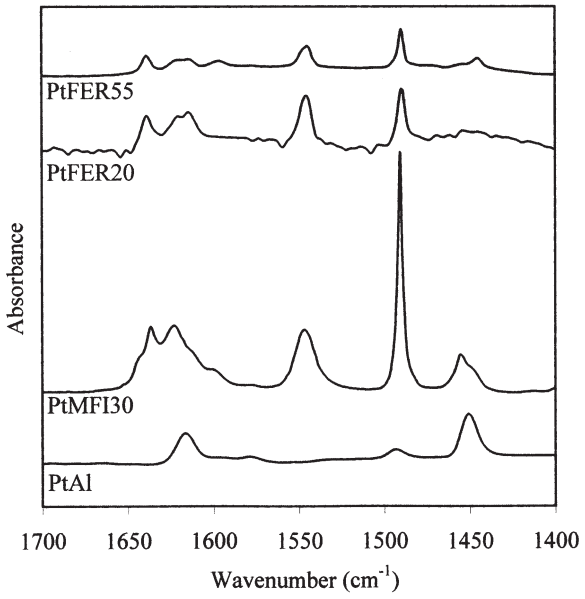

Figure 4. FT-IR spectra after admission of pyridine and subsequent evacuation at 250 °C of the investigated catalysts.

bonded pyridine on Lewis acid sites. These latter bands increase in wave number as the strength of interaction increases, giving an indication of the strength of Lewis acid sites [21]. Figure 4 reports FT-IR spectra of supported platinum samples after admission of pyridine and subsequent evacuation at 250 °C. According to the literature [22], the PtAl sample shows a spectrum with typical bands of Lewis acid sites (1448 and 1614 cm^{-1}) and no band related to Brønsted acidity. Spectra of zeolite-supported platinum samples (PtMFI30, PtFER20 and PtFER55) exhibit bands due to both Brønsted (1544 cm^{-1} and 1636–1642 cm^{-1}) and Lewis (1444–1454 cm^{-1} and 1610–1620 cm^{-1}) acidity [21]. The ratio of Brønsted to Lewis acid sites is sensibly higher on Pt/H-ferrierite samples, indicating that these samples contain predominantly Brønsted sites and rather few Lewis sites. From the figure, it can also be seen that the number of both Brønsted and Lewis sites decreases on increasing the SiO_2/Al_2O_3 ratio of the ferrierite. It is also interesting to note that both Pt/H-ferrierite samples display bands of lower intensity compared to those of the Pt/H-ZSM5 catalyst. This is not in agreement with the results obtained by NH_3-TPD, which, differently, indicate that PtFER20 has a larger number of acid sites compared to PtMFI30 (table 1). This can be explained considering that not all acid sites of ferrierite are easily accessible to pyridine molecules, because of channel size constraints [23].

4. Discussion

The present FT-IR investigation of chlorobenzene and dichlorobenzenes adsorbed on Pt/H-ZSM5 and Pt/H-ferrierite catalysts provides evidence for a different accessibility of these chloroaromatic molecules into

channels of the zeolites (H-ZSM5 and H-ferrierite) used as support. In particular, in the case of the Pt/H-ZSM5 sample, it was observed that the diffusion of *m*-$PhCl_2$ (diameter of 6.8 Å [24]) in the internal sites of H-ZSM5 is more hindered than that of the less bulky *p*-$PhCl_2$ (6.2 Å [25]). A similar behavior has been reported by Busca and coworkers concerning the interaction of xylene isomers with H-ZSM5 [18,19]. This molecular sieving effect of H-ZSM5 is reasonable considering that the structure of this zeolite consists of straight and sinusoidal channels, both formed by rings of 10 oxygen atoms, with openings respectively of 5.3×5.6 Å and 5.1×5.5 Å [26]. The hindrance effect was more evident with Pt/H-ferrierite samples, in agreement with the smaller diameter of ferrierite cavities (4.3×5.5 Å for the larger channels [26]). In this case, in fact, all investigated molecules (PhCl, *p*-$PhCl_2$ and *m*-$PhCl_2$) were not able to enter, at room temperature, the internal pores of ferrierite. The access of PhCl and *p*-$PhCl_2$ was significant only when contact was carried out at high temperature (300 °C), probably due to the increase in the temperature in the intracrystalline diffusivity of these molecules in H-ferrierite pores [27]. *m*-$PhCl_2$, whose diameter is much larger than the window size of the ferrierite, did not enter at all the channels of this zeolite, not even at high contact temperatures.

On the basis of the above FT-IR results, it can be pointed out that chloroaromatics undergo a significant steric hindrance at the mouth of the pores of zeolite crystals. This finding accounts for the different formation of polychlorinated benzenes as by-products during the PhCl oxidation over our supported platinum catalysts. The order of $PhCl_x$ outputs observed (Pt/H-ferrierite < Pt/H-ZSM5 ≪ Pt/γ-Al_2O_3), in fact, fits well with that of the size of pores of the supports used (H-ferrierite < H-ZSM5 ≪ γ-Al_2O_3). Indeed, it must be reminded that active metal particle size has been reported to affect the formation of $PhCl_x$ over Pt/γ-Al_2O_3 catalysts, with smaller platinum ensembles producing more $PhCl_x$ [6]. In our case, however, considering that all samples used in this work exhibit similar platinum particle size (see H/Pt ratio in table 1), this parameter cannot be taken into account to explain the different $PhCl_x$ formation observed. Therefore, it can be suggested that the pore structure of the support has a key role in determining the selectivity to $PhCl_x$ in the oxidation of chlorobenzene over supported platinum systems, the lower the size of channels the more hindered the side reaction of PhCl chlorination to $PhCl_x$.

A further evidence of the hypothesis of a shape selectivity effect induced by the support derives from the analysis of $PhCl_x$ distribution patterns, which show that on Pt/H-ferrierite samples the formation of $PhCl_x$ is limited exclusively to dichlorobenzenes, whereas on Pt/H-ZSM5, together with $PhCl_2$ isomers, small amounts of $PhCl_3$ were also formed. In the case of the Pt/γ-Al_2O_3 sample, considering that γ-Al_2O_3 has an average pore size of 110 Å, no hindrance effect can occur, justifying the high production of $PhCl_x$ as well as the formation of the full spectrum of $PhCl_x$. A molecular sieving effect of the support also agrees with the relative distribution of the $PhCl_2$ isomers observed. In fact, over Pt/γ-Al_2O_3, the distribution of $PhCl_2$ follows the order *m*-$PhCl_2$ > *p*-$PhCl_2$ > *o*-$PhCl_2$, in accordance with a radical mechanism of PhCl chlorination [5,16] and higher reactivity of *o*-position. On the contrary, on Pt/zeolite catalysts *p*-$PhCl_2$, which is the dichlorobenzene isomer with the lowest steric hindrance, is always the most abundant $PhCl_2$.

The oxidation of halocarbons over Pt/oxide systems has been proposed to occur through the adsorption of the hydrocarbon on acid sites of the support and of the oxygen on active metal sites [13,16]. Effectively, FT-IR spectra of adsorbed chlorobenzene showed that both bridging OHs (internal) and terminal silanols (external) of H-ZSM5 (figure 1) and H-ferrierite (figure 2) are perturbed by the interaction with chlorobenzene under reaction conditions. The extent of perturbation of internal OHs is sensibly higher with respect to that of external ones as it can be inferred by comparing the shifts in the frequency of the corresponding OH bands upon adsorption with the organic molecule. This indicates a stronger interaction of PhCl with internal bridging OHs, which are more acidic. Therefore, it can be assumed that PhCl oxidation over Pt/zeolite catalysts involves the adsorption of the reactant on Brønsted acid sites of the zeolite. On the other hand, it has been reported that chloroaromatics can adsorb on Lewis acid sites of oxides through the chlorine atom [28]. This kind of interaction probably occurs in the case of the Pt/γ-Al_2O_3 sample, where no Brønsted sites are present. On the basis of these considerations, it is plausible that support acidity could also affect catalytic performances of alumina and zeolite supported platinum catalysts toward combustion of chlorobenzene. Indeed, we found that Pt/zeolite samples, which exhibited both Brønsted and Lewis acid sites, showed higher activity compared to Pt/γ-Al_2O_3, on which Lewis acidity is exclusively present. Moreover, in the case of Pt/H-ferrierite samples, catalytic activity (figure 3) was found to decrease on increasing the SiO_2/Al_2O_3 ratio, i.e., the number of Brønsted acid sites (figure 4), of ferrierite. The same trend in the activity has been recently shown by us on various Pt/H-ZSM5 catalysts, the higher the SiO_2/Al_2O_3 ratio of H-ZSM5 the lower the activity of the system in chlorobenzene oxidation [16]. Therefore, data reported here indicate that PhCl oxidation rates depend on acid properties of catalyst, the presence of Brønsted acid sites enhancing chlorobenzene conversion. A relationship between activity and strong Brønsted acidity has also been described in the oxidation of aliphatic chlorinated hydrocarbons over H-zeolites [11]. Nevertheless, it is noteworthy that no

significant change in the amount and distribution of $PhCl_x$ was observed when the SiO_2/Al_2O_3 ratio of ferrierite was varied, pointing out that acidity is not responsible for the selectivity to $PhCl_x$. This finding is in accordance with data recently reported by us over Pt/H-β and Pt/H-ZSM5 catalysts [16]. Therefore, results reported in this paper support the hypothesis that $PhCl_x$ formation is mainly controlled by a product shape selectivity effect induced by the crystal structure of the support, a lower size of pores hindering the chlorination of PhCl to noxious $PhCl_x$ and favoring the formation of isomers with lower steric hindrance. The acidity of the support is instead involved in the activation of the reactant molecule (chlorobenzene) and therefore affects the activity of the catalytic system.

5. Conclusions

On the basis of the present FT-IR investigation, it was concluded that the support significantly affects the catalytic performance of supported platinum catalysts toward the chlorobenzene combustion. In particular, it was verified that support acidity is important in directing the activity of the system, whereas the molecular sieving effect of the support has a key role in determining the level and the distribution of polychlorinated compounds formed during the combustion process.

Acknowledgments

The financial support of MIUR (PRIN-2001) is acknowledged.

References

[1] G.H. Hutchings, C.S. Heneghan, I.D. Hudson and S.H. Taylor, Nature 384 (1996) 341.
[2] M.L.H. Green, R.M. Lago and S.C. Tsang, J. Chem. Soc. Chem. Commun. (1995) 365.
[3] J. Spivey, Ind. Eng. Chem. Res. 26 (1987) 2165.
[4] S. Minicò, S. Scirè, C. Crisafulli, R. Maggiore and S. Galvagno, Appl. Catal. B 28 (2000) 245.
[5] R.W. van den Brink, R. Louw and P. Mulder, Appl. Catal. B 16 (1998) 219.
[6] R.W. van den Brink, R. Louw and P. Mulder, Appl. Catal. B 24 (2000) 255.
[7] Y. Liu, M. Luo, Z. Wei, Q. Xin, P. Ying and C. Li, Appl. Catal. B 29 (2001) 61.
[8] Y. Liu, Z. Wei, Z. Feng, M. Luo, P. Ying and C. Li, J. Catal. 202 (2001) 200.
[9] G. Sinquin, J.P. Hindermann, C. Petit and A. Kiennemann, Catal. Today 54 (1999) 107.
[10] S. Krishnamoorthy, J.P. Baker and M.D. Amiridis, Catal. Today 40 (1998) 39.
[11] J.R. Gonzalez-Velasco, R. Lopez-Fonseca, A. Aranzabal, J.I. Gutierrez-Ortiz and P. Steltenpohl, Appl. Catal. B 24 (2000) 233.
[12] R. Lopez-Fonseca, J.I. Gutierrez-Ortiz, M.A. Gutierrez-Ortiz and J.R. Gonzalez-Velasco, J. Catal. 209 (2002) 145.
[13] S. Chatterjee and H.L. Greene, J. Catal. 130 (1991) 76.
[14] L. Becker and H. Forster, J. Catal. 170 (1997) 200.
[15] S. Scirè, S. Minicò, C. Crisafulli, G. Burgio and V. Giuffrida, Stud. Surf. Sci. Catal. 142 (2002) 1023.
[16] S. Scirè, S. Minicò and C. Crisafulli, Appl. Catal. B 45 (2003) 117.
[17] M. Iwamoto, Stud. Surf. Sci. Catal. 130 (2000) 23.
[18] M. Trombetta, T. Armaroli, A. Gutierrez Alejandre, J. Ramirez Solis and G. Busca, Appl. Catal. A 192 (2000) 125.
[19] T. Armaroli, M. Bevilacqua, M. Trombetta, A. Gutierrez Alejandre and J. Ramirez, G. Busca, Appl. Catal. A 220 (2001) 181.
[20] D.H. Whiffen, J. Chem. Soc. (1956) 1350.
[21] J.A. Lercher, C. Grundiling and G. Eder-Mirth, Catal. Today 27 (1996) 353.
[22] C. Morterra and G. Magnacca, Catal. Today 27 (1996) 497.
[23] B. Wichterlovà, Z. Tvarůžkovà, Z. Sobalik and P. Sarv, Microporous Mesoporous Mater. 24 (1998) 223.
[24] G.-q. Guo and Y.-c. Long, Separation, Purif. Technol. 24 (2001) 507.
[25] H. Fu, L.A.F. Coelho and M.A. Matthews, J. Supercrit. Fluids 18 (2000) 141.
[26] D.W. Meier and D.H. Olson, *Atlas of Zeolites Structure Types* (Butterworth-Heinemann, London, 1992).
[27] Y. Fujikata, T. Masuda, H. Ikeda and K. Hashimoto, Microporous Mesoporous Mater. 21 (1998) 679.
[28] M.A. Larrubia and G. Busca, Appl. Catal. B 39 (2002) 343.